

# Hacky Racers: Exploiting Instruction-Level Parallelism to Generate Stealthy Fine-Grained Timers

Haocheng Xiao, Sam Ainsworth  
University of Edinburgh  
{haocheng.xiao, sam.ainsworth}@ed.ac.uk

## Abstract

Side-channel attacks pose serious threats to many security models, especially sandbox-based browsers. While transient-execution side channels in out-of-order processors have previously been blamed for vulnerabilities such as Spectre and Meltdown, we show that in fact, the capability of out-of-order execution *itself* to cause mayhem is far more general.

We develop Hacky Racers, a new type of timing gadget that uses instruction-level parallelism, another key feature of out-of-order execution, to measure arbitrary fine-grained timing differences, even in the presence of highly restricted JavaScript sandbox environments. While such environments try to mitigate timing side channels by reducing timer precision and removing language features such as *SharedArrayBuffer* that can be used to indirectly generate timers via thread-level parallelism, no such restrictions can be designed to limit Hacky Racers. We also design versions of Hacky Racers that require no misspeculation whatsoever, demonstrating that transient execution is not the only threat to security from modern microarchitectural performance optimization.

We use Hacky Racers to construct novel *backwards-in-time* Spectre gadgets, which break many hardware countermeasures in the literature by leaking secrets before misspeculation is discovered. We also use them to generate the first known last-level cache eviction set generator in JavaScript that does not require *SharedArrayBuffer* support.

## 1 Introduction

The disclosures of Spectre [37] and Meltdown [42] in 2018 have moved side channels into the mainstream. Various performance-optimization techniques in today’s processors, such as transient execution, and caches [8, 9, 15, 16, 19, 28, 30, 32, 35, 37, 39, 40, 42, 44, 53, 54, 58, 63, 68, 70, 74, 77, 78, 79, 81, 87, 89, 90], have been shown to be exploitable by attackers to leak or exfiltrate information.

This has particularly manifested in browser security, where large amounts of untrusted sandboxed JavaScript code is executed. Although JavaScript is sandboxed, it is still vulnerable to most architectural attacks, e.g., Spectre [8, 37], Rowhammer [29], *prime+probe* [48] and many others [27, 32, 52, 73, 76, 80]. Still, timing side-channel attacks rely on being able to reliably measure timing differences, and so the precision of the timers provided by browsers’ APIs has been decreasing [7, 47]. Although the level of assurance this mitigation actually gives has been hotly debated [6, 38, 45, 72], vendors still tend to resort to this whenever other more effective mitigations, such as

patching processor microarchitecture, disabling hardware optimization techniques, or process-level isolation [57] are unavailable and/or degrade performance to too high a degree [4, 34, 64, 66, 84, 93].

A prime example of this is that when *SharedArrayBuffer*, a JavaScript multi-threaded language feature, was found to provide an indirect fine-grained timer through counters and thread-level parallelism [69], it was temporarily removed from mainstream browsers [21] as a response to Spectre [37]. It is still blocked in recent mitigation proposals such as Chrome Zero [67], in the Tor Browser [1], and in Firefox and Chrome for websites that have not opted in to cross-site isolation [13].

In this paper we break the illusion of security brought by this timer-coarsening mitigation, and by the removal of *SharedArrayBuffer*. We develop Hacky Racers, a new class of timing gadgets that can be used to measure arbitrary fine-grained timing differences on out-of-order processors without any previously removed or potentially removable language features [21], cross-thread contention [69], or indeed anything other than simple arithmetic operations, branches, loads, and coarse-grained timers.

While attacks such as Spectre [37] depend on the transient-execution capability of an out-of-order processor, and *SharedArrayBuffer* timers on thread-level parallelism that can be disabled, we instead attack instruction-level parallelism (ILP): the ability for two or more data-independent instruction sequences from the *same thread* to execute simultaneously, creating a race for which executes first. The key insight is that an attacker can use ILP to generate sequences of instructions that can be comparatively timed against each other, even in the absence of any direct source of time. The actual execution order between two racing instructions can be converted into long-lasting cache-state changes, such as an L1 eviction or reordering two cache fills, by *racing* (section 5) two different sections of independent code against each other. This can then be *magnified* (section 6) by repeatedly sampling the cache [62] or causing contention in the pipeline, to convert the fine-grained timing difference into a coarse-grained timing difference, undiminished by low resolution or noise.

This paper makes the following contributions:

1. We propose a new method of exploiting out-of-order execution, Hacky Racers, which use instruction-level parallelism to generate fine-grained timers.
2. We introduce *racing gadgets*, used to differentially time one event relative to another, and leave a state accord-

ingly as an input for magnifier gadgets.

3. We introduce *magnifier gadgets*, to amplify the timing difference between different micro-architecture states caused by a small difference, such as a speculative memory access, or the order of two cache fills.
4. We prove the efficacy of Hacky Racers through implementing several attacks in a browser without using *SharedArrayBuffer*, including a new variant of Spectre V1 [37], SpectreBack, that can leak secrets backwards-in-time, to before any misspeculation is discovered.
5. We demonstrate that Hacky Racers can resurrect side-channel attacks thought to have been purged via timer coarsening, by implementing the first known eviction-set generator in JavaScript without *SharedArrayBuffer*.

To be clear, Hacky Racers are not as big a threat as transient-execution attacks such as Spectre [37], as while transient-execution attacks directly leak secrets, Hacky Racers (and instruction-level parallelism in general) instead leak time. Still, that means that Hacky Racers can form the critical part in making information-leakage attacks (such as Spectre) feasible, by making information-recovery of them practical even in extremely restricted environments.

We have disclosed our findings to the Tor Browser, Chrome, Firefox, and Cloudflare. The Hacky-Racers attack code is open-sourced at <https://github.com/FxPiGaAo/Hacky-Racer>.

## 2 Background and Related Work

Here we first introduce how timers are used to facilitate side-channel attacks. We then discuss current methods of timing in browsers and their mitigations, followed by background on the out-of-order execution of modern processors that we use to generate the instruction races used in Hacky Racers. Finally, we discuss Spectre attacks.

### 2.1 Timing in JavaScript Attacks

Timers are typically used in JavaScript attacks in two places: in the receiving stage of a side channel (e.g. to time the presence/absence of a cache line [8] or execution-unit contention [25]), in the last-level cache (LLC) eviction set (EV) profile stage [22, 29, 48, 52, 53, 75, 83, 91] (to allow efficient preparation of the cache before an attack), or both.

The precision of the timer matters when the attacker needs to time the access latency to one or multiple addresses to distinguish whether a cache miss exists or not. Last-level-cache (LLC)-based channels [30, 48, 67], such as *Flush+Reload* [92], *Prime+Probe* [43, 49, 51, 72], *Evict+Time* [49], *Evict+Reload* [30], *Reload+Refresh* [18, 87] and *Evict+Prefetch* [28], are prevalent, since they are still effective even if the attacker and victim never share the same core. Though the timing of an LLC miss, which is used in the eviction-set profiling and the secret transmission stage, is more coarse grained than an L1 cache miss, its timing difference is still around 100ns, and so cannot be timed natively with the coarse-grained timers (section 2.2) in today's browsers.

A precise timer is critical to some other (non-timing-side-channel) attacks, such as rowhammer.js [29] and

Spook.js [8], as they also require LLC eviction-set profiling to actively trigger victim cache misses from the attacker's side. Finally, there are other side-channel attacks that require timing information such as website fingerprinting [48, 59, 72, 73], inferring neural-network architectures [89] and breaking AES [32].

### 2.2 Timers in Browsers and Mitigation

Sources of time in browsers can be generated intentionally by APIs, or unintentionally by other system behavior [61, 69].

**Performance.now()** is the most precise timer provided natively by browsers' APIs. Its precision has changed over time as a response to attacks. For example, its resolution was decreased to  $5\mu\text{s}$  in both Chrome and Firefox in 2015 as the first browser side-channel attack [48] emerged. In early 2018, Spectre [37] forced vendors to further decrease its precision to 2ms in Firefox 59, and 100ms in Chrome with a 100ms jitter [61]. After site isolation [57], a mitigation to remove secrets from the address space, was added in Chrome and Firefox, the precision restriction was loosened to  $5\mu\text{s}$  plus jitter in Chrome [7] and  $5\mu\text{s}$  in Firefox [46] within the same origin<sup>1</sup>.

**SharedArrayBuffer** was introduced by ECMAScript 2017 [31] to facilitate cross-thread communication. It provides shared memory between multiple workers, enabling simultaneous data reading and writing between threads. Based on this feature, Schwarz et. al. [69] built a high-resolution timer with precision around 2 - 15 nanoseconds. A shared value among a main thread and a subthread is allocated in this *SharedArrayBuffer*. The subthread serves as a counting thread, incrementing the value continuously in an infinite loop. The main thread then gets timestamps by reading the value.

Similar to the high-resolution `performance.now()` API, the *SharedArrayBuffer* feature was also disabled [3] as a response to Spectre [37] and re-enabled after the implementation of site isolation in Chrome and Firefox only for cross-origin isolated pages [13]. It is still disabled in Tor [2] and Chrome Zero [67].

**Others** Apart from lowering precision, other countermeasures have been proposed, such as fuzzy timers [38, 82] and limiting shared memory and message passing. In fuzzy time, the clock edge is randomly perturbed, further reducing the final observed precision. This was thought to mitigate the edge-thresholding technique [69], which otherwise has the potential to recover the resolution by adding extra instructions to reach the threshold.

### 2.3 Repetition and Magnifier Gadgets

To observe fine-grained timing difference with a coarse-grained timer, the signal must in some way be amplified. Here we divide such methods into two categories: *repetition gadgets*, which repeat the attack many times, and *magnifier gadgets*, which require the attack to be performed only once.

Repetition gadgets repeat the whole extract-then-transmit process to accumulate the timing difference from each iteration. For example, Skarlatos et al. [74] denoise their SGX attack by repeatedly triggering replay on illegal instructions

<sup>1</sup>Resolution can also be customized to a larger value by enabling `privacy.resistFingerprinting` [47] in Firefox, and  $100\mu\text{s}$  (from the default  $5\mu\text{s}$ ) in non-isolated contexts in Chrome.

without actually incurring a page fault. McIlroy et al. [45] propose a gadget to create timing difference for Spectre gadgets [37] that can be observed by the coarse-grained timer in a browser, by repeatedly triggering the attack. Schwarzl et al. [71] implement a similar attack on Cloudflare Workers [5], the serverless execution framework, where timing can only be achieved by a remote timing server. However, repetition on its own has the risk of cancelling out the timing difference between different stages (section 7.1).

In contrast, a magnifier gadget first extracts and transmits the secret into state differences once, and then executes instructions that both maintain the state difference and accumulate the timing difference at the same time. Therefore, this gadget will not suffer from noise from stages such as branch mistraining. We repurpose the magnifier gadget introduced by the leaky.page Spectre attack [62], which attacks PLRU caches, to time arbitrary sequences of instructions, and introduce new magnifier gadgets that avoid any transient execution, and work for other cache replacement strategies (section 6).

Orthogonally, attackers can also leave multiple state differences [86] after the secret is extracted once, which can also increase the timing difference by a constant (typically limited) multiple – though further timer coarsening by a similar constant can mitigate the effects.

## 2.4 Out-of-Order Execution

Out-of-order execution is an almost ubiquitous [37] processor microarchitectural optimization technique, designed to exploit instruction-level parallelism, by executing many independent instructions from the same thread simultaneously when there are no data dependencies between them. This optimization must obey the programmer’s sequential view of execution, and so instructions commit in-order at the back-end of the pipeline. Still, the true out-of-order nature of execution may still leave traces in structures outside the programmer’s model, such as the cache, which we can pick up to infer which executed first.

In this paper, we define a *path* (section 4) as an instruction sequence that currently does not have any external data dependence, and could thus be processed independently of any instructions outside of that sequence. This independence allows execution to flow within separate paths simultaneously.

## 2.5 Speculative Execution Attacks

To find useful work, an out-of-order processor must speculate on the future flow of instructions, such as via branch predictors. This incorrect execution will be rolled back, but may still leave traces that can be found by an attacker.

Misspeculated (or transient) execution was famously attacked by Spectre [37]: the branch predictor or branch target buffer can be poisoned to cause incorrect instructions (such as out-of-bounds accesses to arbitrary parts of the address space) to execute speculatively, and leave traces in the cache. Meltdown [42] similarly attacked the behavior of some Intel cores to incorrectly forward on the values of exceptional loads to other transient instructions.

Hacky Racers are different. Though transient execution makes the construction of its gadgets simpler, the attack requires no transient execution at all. The *correct* execution of

instructions<sup>2</sup>, executed in the wrong order, is still a threat to browser security. Hacky Racers also provide new perspectives on transient execution attacks. In section 7.3, we will show new racing gadgets that allow leaking of data in ways that many proposed mitigations cannot eliminate. Many other speculative execution attacks based on contention, of either arithmetic logic units (ALUs) in the core [25] or miss status holding registers (MSHRs) in the cache [15], could also be validly formulated as Hacky Racers racing gadgets.

## 3 Threat Model

We assume an arbitrary side-channel attack in a JavaScript application, such as an advertisement in a web browser trying to access secrets outside its sandbox, that needs to time one or several operations in order to succeed, such as the probe operation in a prime+probe [51]. We further assume that the timing difference brought about by this side channel is fine-grained – of the order of 100 nanoseconds or smaller, thus cannot be observed by current browsers’ JavaScript native timers. We also assume the attacker can execute any valid JavaScript code within their sandbox, but that any timers or other forms of time (section 2.2), are limited to  $5\mu s$  granularity. The majority of our attacks also work for as coarse a granularity as has ever been introduced in a browser (100ms) and higher, but we use  $5\mu s$  as the threshold for success of an attack. We do not require the attacker to have access to any cross-thread primitives. The attacker will succeed if they are able to measure this difference and thus construct an information channel. This gives Hacky Racers the potential to resurrect or accelerate attacks that were previously hindered by timing obfuscation [38, 67].

We assume the attacker is executing on a processor with out-of-order execution, as is typical on modern devices [37], able to execute tens-to-hundreds of instructions into the future. The instruction length of operations to be measured is limited by the reorder buffer of a processor in practice. However, we find that very few concurrently executing instructions are required for success.

Our threat model could also be expanded to other environments where a fine-grained timer is unavailable, such as Cloudflare Workers [5] and, Apple M1 processors and other ARM systems [41, 56]. We leave these to future work for simplicity.

## 4 Path Construction

Here we define *paths* as a unit of simultaneous execution *within* a single thread (exemplified in fig. 1) on an out-of-order processor. Between two independent paths  $path_a$  and  $path_b$ , there must be no data dependencies, and thus they may execute entirely in parallel with each other on an out-of-order processor. Likewise, no instruction within the path should be data dependent on any instruction outside the path, except for instructions that come before the entire path in program order. Within a path, there may be one or more *chains* which are connected via data dependence,

<sup>2</sup>Concurrent to this work, Rokicki et al. [60] also exploited ILP to build a port-contention channel in JavaScript that can be used to determine a user’s CPU model. Their attack can be used to replace the simultaneous multi-threading (SMT) feature relied by the original attack with ILP contention, but still uses a *SharedArrayBuffer* based timer, which Hacky Racers can replace.

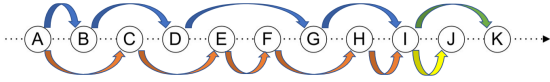


Figure 1: Paths within instructions. Instructions are placed in program order on this dotted timeline. Data-dependence is indicated as arrows, and is colored in group of paths. When instruction A’s result is ready, two independent *paths* could execute in any order: {B, D, G} and {C, E, F, H}.

such that no two instructions within each *chain* can execute simultaneously or out-of-order. Note that *paths* are defined in order to simplify and reason the construction of our Hacky Racer, and there could be multiple combinations to separate one instruction sequence into *paths* while only one of them is meaningful.

We first introduce the construction process of *paths* that satisfy the synchronization and concurrency requirements of Hacky Racers. We then demonstrate how to embed the expression whose timing we would like to observe, named the *target expression* or  $Expr_1$ , into a path as the first step of our Hacky Racer.

Ultimately, this path will compete against another path, the *baseline path*, as part of the *racing gadgets* of section 5, which transform the race result of the two paths into a state change in the system. This state change can then be input into magnifier gadgets to amplify the side channel to something observable via coarse-grained timer, even after only a single attack instance.

#### 4.1 Path Synchronization

Code listing 1 shows an example of a construction of two independent paths,  $path_a$  and  $path_b$ , that are eligible for execution simultaneously. In this example, each path consists of a single chain. To synchronize their starting execution, we ensure the first instruction in the chains in both paths have a common data dependency, in instruction A<sup>3</sup>. We ensure that instruction A, loading  $Array[0]$ , will incur a cache miss that delays executions of both paths to avoid frontend fetch/decode contention, meaning all instructions will have reached the out-of-order backend by the time any is eligible for execution. As a result,  $path_a$  and  $path_b$  start at the same time and run in parallel.

#### 4.2 Expression Embedding

In addition to synchronizing the start of each path’s execution, to observe the execution timing of the *target expression*, it should be embedded into a single path, named the *measurement path*. The path may also be required to end with an attacker-defined result as its *terminator instruction*, transitively dependent on the final instruction of every *chain* within the path. In practice this terminator instruction will serve either as a branch-condition variable or as a data-access index, to be used as a side channel to infer their relative timing, as will be introduced in section 5. To satisfy these two restrictions, we construct both a *pre-extension* and *post-extension* around every chain within the original *target expression*. The

<sup>3</sup>Where paths have multiple chains within them as in figure 2, the first instruction in every chain must depend (transitively) on this common dependency.

```

1 function myFunction() {
2   var A = array[0];
3   var B = arrayA[A]; //path A
4   var C = arrayB[A]; //path B
5   var D = arrayA[B]; //path A
6   var E = arrayB[C]; //path B
7   var F = arrayA[D]; //path A
8   var G = arrayB[E]; //path B
9   var H = arrayA[F]; //path A
10  var I = arrayB[G]; //path B
11  var J = H + I;
12  return J;
13 }

```

Code Listing 1: An example for two synchronized paths. These form two independent chains of operations that will run concurrently on an out-of-order processor: knowledge of which finishes first can be used as a side channel.

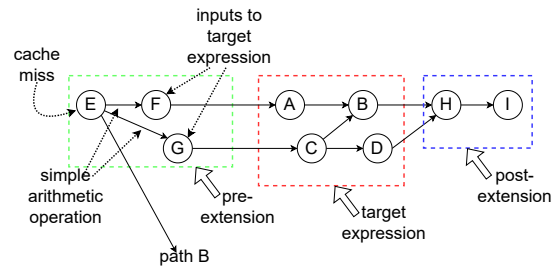


Figure 2: The *target expression* to be measured is embedded into a path. *Pre-extension* and *post-extension* instructions are shown in the green and blue box, wrapping the target expression. Instruction E, the beginning of the path, will incur a cache miss, and be depended by  $path_b$ .

*pre-extension*’s output encodes the input data for the *target expression*, ensuring that all data inputs to the function depend on a single *head instruction* at the start of the path, while the *post-extension* converts the original outputs of the *target expression* into inputs to an attacker-controlled instruction, to ensure that this instruction only executes following the completed execution of all outputs.

In our example, The *target expression* is shown both in the red-dotted box of figure 2 and in the *OriginFunc()* of code listing 2. The transformed function contains the *measurement path* transformed from the *target expression*. Between the *pre-extension* and *target expression*, the indices used to load A and C in the *OriginFunc()* are replaced by F and G, which encode each index as a data dependency of E. As is discussed in section 4.1, the load of E will suffer a cache miss to synchronize the starts of the two paths. In the *post-extension*, var H is created to depend on both B and D, ensuring the completion of the whole path only after B and D have finished execution. Finally, in var I, an offset is added to H to achieve the desired output (for example, the access of a specific cache line, or branch condition, to create the side channel that indicates completion). Thus, the *target operation* is embedded into a path that produces a particular output only once the full operation has completed. In the next section, we will describe how to synchronize it against a competing path, by using this chosen output as a side channel to infer ordering between the two paths.

```

1 function OriginFunc(x, y) {
2   var A = array[x];
3   var C = array[y];
4   var B = array[A+C];
5   var D = array[D];
6   return B + D;
7 }
8
9 //construction of path A
10 function TransformedFunc(x, y) {
11 //pre-extension
12   var E = array[0]; //E = array[0] = 0
13   var F = E + x; //F = x (input 1)
14   var G = E + y; //G = y (input 2)
15
16 //modified target expression
17   var A = array[F];
18   var C = array[G];
19   var B = array[A+C];
20   var D = array[D];
21
22 //post-extension
23   var H = B + D; //depends on both outputs
24   var I = H + delta; //I = attacker-predefined
25
26 //path B is omitted here, which also depends on E
27   ...
28   return;
29 }

```

Code Listing 2: The corresponding code example for fig. 2, where the **target expression** is embedded into a path. *OriginFunc()* is the target expression, while the *TransformedFunc()* is the transformed version, with *pre-extension* to cause both Paths in OriginFunc to run simultaneously, and *post-extension* to leave a microarchitectural trace that can be picked up as the unique end of the target expression.

## 5 Racing Gadgets

We develop *racing gadgets* to measure timing *relatively* with reference to a *path* with a known constant execution time, which we call a *baseline path*,  $path_b$ . The target expression to be measured,  $Expr_t$ , is placed in the *measurement path*,  $path_m$ , starting at the same time as the *baseline path*. Thus, the *path* with a shorter execution time will finish first. This *completion order* between these two *paths* leaves a microarchitectural difference that will serve as the input of the *magnifier gadget*.

### 5.1 Transient Presence/Absence (P/A) Racing Gadget

This gadget converts the *completion order* into whether there is a transient cache access to a specific address or not. This is achieved by altering how quickly a mispredicted branch is corrected, depending on the operation time that we are interested in. The cache-state change caused by the transient access serves as input to the corresponding *magnifier gadget*.

Assume  $T$  is threshold which we would like to distinguish whether the execution time of  $Expr_t$  is larger or smaller than. We prepare two operation sequences  $path_m(Expr_t, x)$  and  $path_b()$ <sup>4</sup>. The variable  $x$  controls the final data output of  $path_m$ .  $path_m(Expr_t, x)$  satisfies the following requirements:

<sup>4</sup>The construction to satisfy these restrictions is discussed in section 4.

- a)  $path_m(Expr_t, 0) = 1$  and  $path_m(Expr_t, 1) = 0$ .
- b) previous execution of  $path_m(Expr_t, 0)$  will not affect the execution time of  $path_m(Expr_t, 1)$ .

Requirements a) and b) are needed due to the training phase, since its output serves as a condition variable to trick the branch predictor into executing transient code. We set  $x = 0$  during the training phase and  $x = 1$  during the detection phase.

- c)  $Time(Expr_t)_{low} < T < Time(Expr_t)_{high} \Rightarrow Time(path_m(Expr_t, 1))_{low} < T' < Time(path_m(Expr_t, 1))_{high}$

Requirement c) converts the execution-time comparison between  $Expr_t$  and  $T$  into one between  $path_m(Expr_t, 1)$  and  $T'$ , where  $T'$  accounts for the extra time taken in *pre-extension* and *post-extension*.  $Path_b()$  is generated so that its execution time is constant and equal to  $T'$ , so that the race can distinguish whether  $Time(Expr_t)$  is *high* or *low*.

- d) No instruction in  $path_b()$  can have a data dependency on any instruction in  $path_m(Expr_t, 1)$ , and vice versa
- e)  $path_b()$  and  $path_m(Expr_t, 1)$  should be started at almost the same time.

Requirement d) is implied by the definition of *path*, and is necessary to allow the two paths to execute independently (and thus race against each other), while requirement e), to make the race between the two fair (and thus increase precision), is satisfied by letting the first instruction in both paths to be dependent on the same cache miss (section 4.1).

Finally we construct the timing gadget as follows ( $\mapsto$  indicates that  $access[A]$  has a data dependence on the result of  $path_b()$ , thus it will be executed after all of the instructions in  $path_b()$  have executed even on an out-of-order processor):

```

if(path_m(x))
  path_b()  $\mapsto$  access[A];

```

Before this gadget is executed, we train the branch predictor through executing this code snippet with  $x = 0$ . When we execute it with  $x = 1$ , the mispredicted  $path_b()$  will be executed in parallel with  $path_m()$  until one finishes. If  $Time(Expr_t) > T$ , the memory request of  $access[A]$  will be sent after  $path_b()$  finishes before  $path_m()$ . Otherwise when  $path_m()$  finishes first, it will roll back before it reaches  $access[A]$ .

### 5.2 Non-transient Reorder Racing Gadget

Here we introduce another *racing gadget* that does not rely on transient execution, unlike Spectre [37]. No misspeculation is required for this gadget, so it is unaffected by hardware mitigation schemes for Spectre [10, 88, 94] and demonstrates that we are attacking a fundamentally different property of out-of-order execution. Here, inspired by a gadget used as part of speculative interference attacks [15] to defeat invisible transient caching mechanisms for Spectre resistance [88], we convert *completion order* into the *relative order* of two memory accesses, A and B. We construct the gadget as follows:

```

path_m()  $\mapsto$  access[A];
path_b()  $\mapsto$  access[B];

```

And with the following requirements:

- a)  $Time(Expr_i)_{low} < T < Time(Expr_i)_{high} \Rightarrow Time(path_m(Expr_i))_{low} < T' < Time(path_m(Expr_i))_{high}$   
 b) No instruction in  $path_b()$  can have a data dependency on any instruction in  $path_m()$ , and vice versa  
 c)  $path_b()$  and  $path_m()$  should be started at the same time.

These are similar to those of the transient P/A racing gadget except that the first two restrictions are removed, as this gadget does not include branches. Because  $path_b()$  and  $path_m()$  start execution simultaneously, the one which completes first will issue the subsequent memory access earlier than the other.

## 6 Magnifier Gadgets

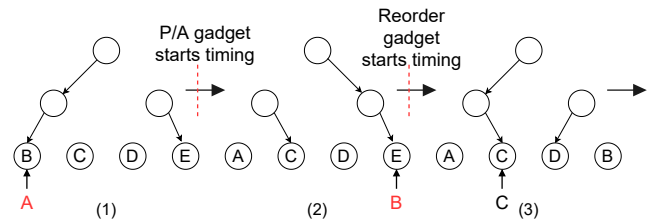
The *racing gadgets* of Section 5 place the system in one of two different micro-architectural states: one to transmit a 1, the other to transmit a  $0^5$ . This state difference serves as the input of the *magnifier gadget*. Our magnifier gadgets use this state as input to create a cascading time difference, typically (but not exclusively) by creating a large number of cache misses for one of these two states, and a large number of cache hits for the other. We first introduce two methods to compose a magnifier gadget in a (widely used [33]) tree-based pseudo-last-recently-used (PLRU) L1 cache – one for the P/A transient racing gadget, and one for the reorder-based non-transient gadget. Finally, we illustrate magnifier gadgets on both a cache with arbitrary replacement policy, and one not using the cache at all – showing that changing the replacement policy is no cure for Hacky Racers, even if specific policies may make the gadgets faster and simpler to implement.

Note that our *magnifier gadgets* simply transform a particular *state difference* to a large *timing difference*; this is not limited to being from the output of the *racing gadgets* from section 5. Indeed, the first gadget is taken from a Spectre attack [62] in the literature, which generates the state difference directly. Rather, the *racing gadgets* are used to convert *arbitrary expressions* to a particular state-change format, as input to a given magnifier. This generic timing capability can manifest in subtle ways: for example in section 7.4, where a racing gadget allows us to convert a last-level cache side channel into an L1-cache side channel, thus allowing us to use an L1-cache magnifier and thus demonstrate the first eviction-set generator in JavaScript without SharedArrayBuffer.

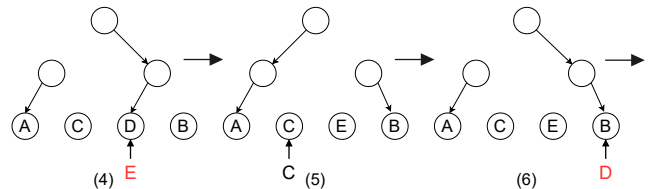
### 6.1 PLRU Gadget for Presence/Absence (P/A) Input

This first magnifier gadget is inspired by Röttger and Janc [62], who used a similar strategy as part of the leaky.page proof-of-concept of a Spectre V1 JavaScript attack. We repurpose it to time arbitrary execution. It utilizes the tree-based Pseudo-Least-Recently-Used (PLRU) [33] cache replacement policy, prevalent on modern CPUs [62], to amplify the timing difference of a single victim access. PLRU policies implement a binary tree structure to approximate a Least Recently Used (LRU) replacement policy. For a clear illustration, we take the PLRU cache’s set associativity  $W = 4$  as an example, and assume all of the following accesses are mapped into the same cache set. As is shown

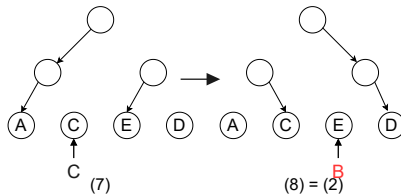
<sup>5</sup>More generally, this may be N different states.



(a) The initial cache state is shown in fig 3.1. Before A was accessed, B was the eviction candidate (EVC), and thus is replaced by A. The pseudo-LRU state is flipped down the accessed path, causing the EVC to switch to E (fig 3.2). In fig 3.3, since access C is a cache hit, nothing is evicted, however the EVC still changes, flipping the arrows down the accessed path between it and fig 3.4.



(b) After accessing E in fig 3.4, A becomes the new EVC (fig 3.5). Since we want to keep A in the cache to allow repeated measurement, C is accessed next, making B the new EVC in fig (3.6), causing D to evict B rather than A.



(c) Since A becomes the EVC again in fig 3.7, C needs to be accessed again to flip the pseudo-LRU state at the top of the tree. Now both the cache state and the access pattern go back to that in fig 3.2, allowing the sequence to be repeated indefinitely without a new access to A.

Figure 3: Cache replacement state and data changes caused by each access of the PLRU Gadget for both 1) *Presence/Absence Input* (section 6.1) when access A is present, and 2) *Reorder Input* (section 6.2) when A is inserted before B. If A is in the cache in the former case, or inserted before B in the latter case, the accesses to B, D and E will repeatedly miss, and the access to C repeatedly hit, and yet the PLRU state prevents them from ever evicting A. The timing starts at the beginning of the corresponding magnifier gadget. Each leaf node represents a cache line in the set and data in it. The arrows within each sub-figure composes one path from root to the leaf, pointing to the eviction candidate. The access pattern and the cache states repeat in a period of 6 accesses, as is shown in (2) - (7).

in figure 3, each leaf node represents a cache line within that set, and the letter within that node indicates the data currently filled in that line. Cache misses are marked in red and those arrows from the root to the leaf always composes one path pointing to the eviction candidate. Every time an access happens to a specific location within that set, it will flip arrows on its path.

The idea behind this gadget is that if the target memory address is brought into the cache by the racing gadget, it will be kept in the L1 cache for the entire magnifier gadget, such that the observed capacity of the set (in timing terms) is less by one than the elements of the following access pattern. Here we construct the access pattern to be a repetition of

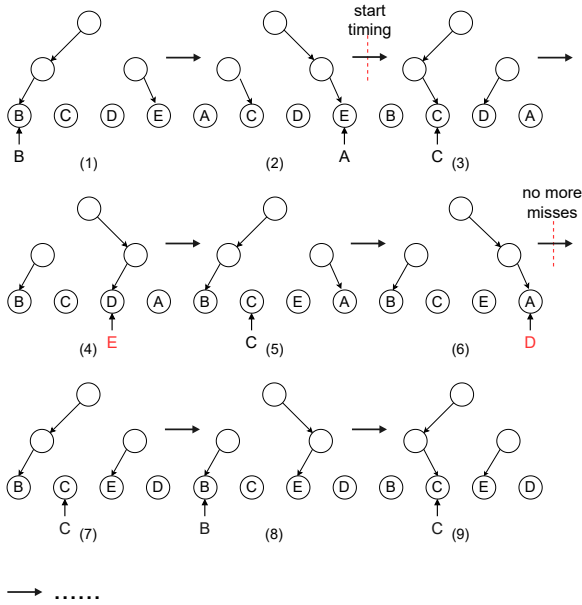


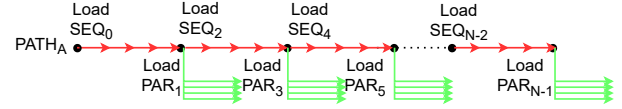
Figure 4: Cache state changes caused by each access of PLRU Gadget for P/A Input. Here B is inserted before A as is shown in the first two subfigures. A is evicted at (6), thus no more misses after that.

four locations: (B, C, E, C, D, C). If A is absent from the cache, no miss will occur. If it is present, the PLRU gadget will never evict it, and thus the cache state and the access pattern will repeatedly go back to the previous state in figure 3.8, forming a cycle from figure 3.3 to 3.8. Therefore, cache misses happen every other access, as is shown in figures 3.2, 3.4, and 3.6.

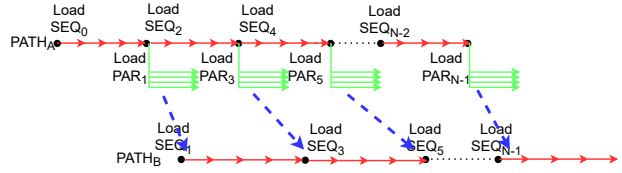
## 6.2 PLRU Gadget for Reorder Input

This gadget takes advantage of the fact that A will be put in different locations within the cache set based on whether A or B is accessed first. As a result, A will always be kept in the cache if A arrives *before* B, and yet will be evicted if A arrives *after* B. Similar to the PLRU gadget for P/A input, the occupation of A will result in a series of cache misses, while the absence of A will present a series of hits, from a sequence of accesses not involving A.

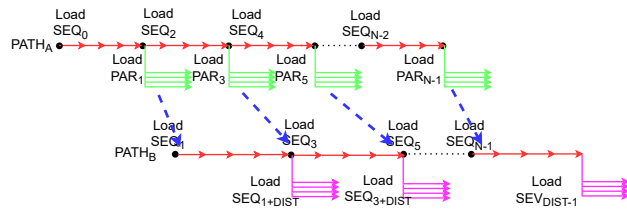
The following accesses pattern is a repetition of (C, E, C, D, C, B). Figure 3 and 4 contrast the cache states of two different relative orders between A and B during the execution of the magnifier gadget. Both start with the same initial state, but proceed differently depending on how A and B are reordered. When A is accessed before B, the state-change flow is the identical to that in the P/A PLRU gadget, despite requiring no transient execution and thus meaning the racing gadget accesses exactly the same cache lines regardless of transmitted signal. The difference is subtle: B in the Reorder Input magnifier gadget is a part of the racing gadget, whereas it is part of the magnifier gadget in the P/A version. By contrast, when B is accessed first, A will be evicted after several accesses, as is shown in fig. 4. After that, there will be no more cache misses, since all following accesses fit into the cache.



(a) The timeline of two paths when no interference occurs.



(b) The execution timeline of both paths when  $Path_A$  starts earlier. The blue arrows indicate that the previous load evicted one data in the eviction set from that cache set. Thus, the loading time of  $SEQ_i$  in  $Path_B$  is longer than that in  $Path_A$ .



(c)  $Path_B$  prefetches for itself, to allow the magnification process to reuse the L1 cache sets cyclically and indefinitely.

Figure 5: The arbitrary-replacement-policy magnifier gadget. The magnifier is itself made up of two racing gadgets,  $Path_A$  and  $Path_B$ , still both within the same thread. Different cache interference, based on whether one starts before the other, cascades into a succession of interference across the entire eviction set. Further, by allowing  $Path_B$  to prefetch for itself in parallel with its loading of the sequential  $SEQ_i$ , the chain reaction can be continued indefinitely.

## 6.3 Arbitrary Replacement Gadget for P/A Input

To demonstrate that changing the replacement policy will not eliminate this exploit, we introduce another *magnifier gadget* for caches with an arbitrary replacement policy within each set. This gadget also utilizes ILP, using a chain reaction to amplify the timing difference of probabilistic state changes across many sets, rather than only converting the timing difference into a deterministic cache state change.

The basic strategy involves the magnifier gadget *itself* becoming a racing gadget, with two paths that exhibit no contention when closely aligned in execution time, and heavy contention when misaligned (e.g. due to the unavailability of an input delaying one path). Once these paths become misaligned, each repetition stays misaligned, multiplying the delay for each stage to complete.

To simplify the demonstration, in the following we focus on an L1 cache with 64 sets, 8 ways and a random replacement policy [14].

The attacker first prepares the initial cache state across  $N$  ( $N < 64$ ) chosen sets, with  $W$  ways per set. The number  $N$  is linear to the final timing difference achieved, limiting the magnification achievable through sets alone, but we also develop a prefetching mechanism to further magnify this timing difference indefinitely. Two paths,  $Path_A$  and  $Path_B$ ,

are generated in the attacker’s code. We define both  $SEQ_i$  and  $PAR_i$  to each be subsets of addresses within the eviction sets of the  $i$ th cache set, without overlap between them.  $PAR_i$  should be sized such that bringing its elements into the cache should evict at least one member of  $SEQ_i$ .

Before  $Path_A$  or  $Path_B$  start, we fill the  $N$  chosen sets with data from  $SEQ_i$ , ensuring that every element of  $SEQ_i$  is within the cache<sup>6</sup>. The memory-access pattern in  $Path_A$  and  $Path_B$  is shown in figure 5a. When  $i$  is odd,  $SEQ_i$  is accessed by  $Path_B$ . When  $i$  is even,  $SEQ_i$  is accessed by  $Path_A$ , followed by  $PAR_{i+1}$ . Arrows in figure 5a represents the data dependence that partially restricts the actual access order during runtime. For example, memory accesses within  $SEQ_0$  are executed sequentially, while the accesses within the  $PAR_1$  that immediately follow can be issued after the last access in  $SEQ_0$ , in parallel with each other. This access pattern ensures that the critical path of both  $Path_A$  and  $Path_B$  is only constructed from accesses in  $SEQ_i$ , as the  $SEQ_i$  accesses will all hit in the cache, and so both paths should finish at approximately the same time when there is no interference between them.

By contrast, consider the timeline shown in figure 5b, when  $Path_A$  starts earlier than  $Path_B$ . By the time  $Path_B$  starts loading  $SEQ_1$ ,  $Path_A$  has already accessed memory from  $PAR_1$ , which (potentially randomly) evicts elements in  $SEQ_1$ . Thus, one or several cache misses will occur when accessing  $SEQ_1$ . While the precise number of misses depends on the replacement policy, this will then delay the start of  $SEQ_3$ , which means that  $Path_A$ ’s  $PAR_4$  will create misses in  $Path_B$ ’s  $SEQ_4$ . This delay accumulates over multiple rounds, with each round with a successful miss increasing the delay.

### 6.3.1 Path prefetching

As the number of cache misses induced in figure 5b is linear to the number of cache sets, the amplification rate is limited, and so timers of coarser granularity would mitigate the attack mechanism. To succeed in spite of these, we can reuse the finite number of cache sets to generate theoretically unlimited timing difference, by generating a *cycle of prefetches* (looping through  $SEQ_i$ ) within the paths to reformulate the initial conditions that caused the timing difference.

Specifically, because the initial cache state is destroyed after being accessed by  $PAR_i$  from  $Path_A$  in both the case of figure 5a and 5b, we add parallel prefetch instructions on  $Path_B$ ’s non-critical path with a prefetch distance  $DIST$ , as is shown in figure 5c. These may be either software prefetch instruction or standard loads – neither will block the out-of-order pipeline, and so neither will affect the execution time of  $Path_B$ ’s critical path, save for the intended interference<sup>7</sup>. This prefetching prepares the initial state for sets that will be later accessed by  $Path_B$ .

### 6.3.2 What if $Path_A$ runs too far ahead of $Path_B$ ?

As there is no data dependence between the two paths, in figure 5b and 5c  $Path_A$  could execute far ahead of  $Path_B$  as time goes by since there is no miss in its critical path.

<sup>6</sup>Even with random replacement, this initial state can be achieved through repeatedly accessing  $SEQ_i$ , provided  $SEQ_i$  is smaller than the set size.

<sup>7</sup>Note that a software prefetch, especially if marked as non-temporal, might be inserted into ways that are easier to be evicted, making the timing difference easier to accumulate [91].

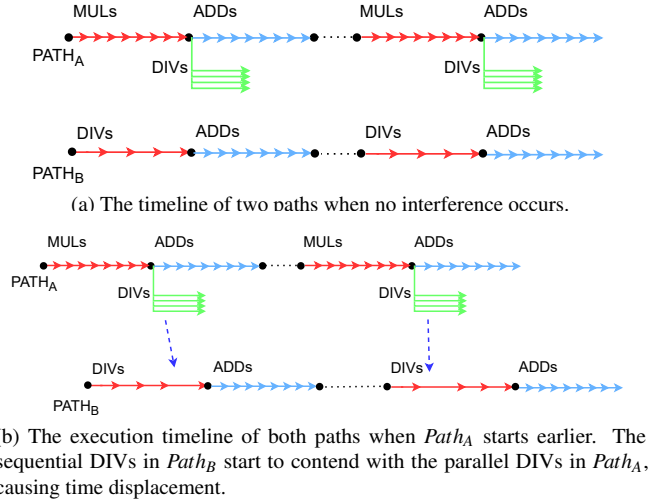


Figure 6: The arithmetic-operation magnifier gadget.

Although this could cause a processor stall as instructions from  $Path_A$  and  $Path_B$  fill the reorder buffer, it has little effect on the final timing. This is because the slower path,  $Path_B$ , continues execution during the stall, and  $Path_A$  will still run ahead of  $Path_B$  after the stall ends. Likewise,  $Path_A$  starting too early has the same effect as both starting at the same time; due to limited ROB capacity,  $Path_A$  cannot run ahead enough in this case to cause interference from different stages.

### 6.3.3 How many number of accesses should be included in each $SEQ_i$ and $PAR_i$ ?

Larger sizes of  $SEQ_i$  and  $PAR_i$  will bring higher chance of cache misses, provided  $SEQ_i$  fits in the cache. We found that for a random replacement policy, with  $SEQ_i$  set to 6 accesses (three quarters the associativity), 5 addresses in  $PAR_i$  was sufficient to provide at least 1 cache miss in  $SEQ_i$  with a 96% chance, with larger values of either increasing the chance to near certainty. A failure to achieve a cache miss, beyond the first round, does not cause the attack to fail: it only causes a single round to not add any further delay. The subsequent round will still be delayed if any previous rounds were, and so will still be able to magnify the delay further.

## 6.4 Arithmetic-Operation-Only Gadget for P/A Input

Although it is possible for previous *magnifier gadgets* to succeed on cache-based channels, we provide a further gadget that makes no use of the cache whatsoever. Since this gadget is composed of arithmetic operations, it eludes any arbitrary form of cache defence.

Similar to the gadget in section 6.3, chain reaction and ILP are also exploited in this gadget by composing two paths,  $Path_A$  and  $Path_B$ . The difference is that sequential accesses are replaced by sequential arithmetic operations, and the contention in cache capacity is replaced by contention in not-fully-pipelined functional units (e.g. dividers). This magnifier is somewhat inspired by SpectreRewind [25] and Speculative Interference [15], which use arithmetic-unit contention to generate Spectre side channels. However, here we



repurpose such contention to generate much larger timing differences from a state generated via racing gadget: thus rather than a single timing difference, we must spawn a chain reaction.

As is shown in figure 6,  $Path_A$  is constructed by chained integer multiply operations (MULs), chained integer add operations (ADDs) and parallel floating point divide operations (DIVs), while  $Path_B$  is constructed from chained DIVs and ADDs. Without contention, the latency of each arithmetic operation is fixed. For simplicity, we assume  $Latency_{DIV} = 9$  cycles,  $Latency_{MUL} = 3$  cycles and  $Latency_{ADD} = 1$  cycles. The MUL and DIV operations serve as the racing stage, while the ADDs serve as a buffering stage.

When both paths starts execution at the same time in figure 6a, we would like the racing stage to finish at the same time. Since the latency of each DIV is three times that of a MUL, we set the number of MUL operations three times that of DIV. Therefore, the parallel DIVs after the racing stage in  $Path_A$  will not delay the execution time of that in  $Path_B$ . In addition, we set the number of ADDs in each ADD chain to be the same as each other, and large enough so that the next racing stage will start at the same time, after all parallel DIVs have finished executing. As most CPUs can execute at least two ADDs at the same time, there is no interference within this buffer stage.

In contrast, figure 6b shows how contention cascades when  $Path_B$  starts later. Since the execution time of their racing stages is the same, the parallel DIVs are issued before  $Path_B$ 's DIVs complete, and thus the two paths compete for resources. This results in  $Path_B$  starting the ADD buffering stage later. As the number of ADDs is the same in both paths,  $Path_B$  will then propagate this increased delay into the next racing stage against  $Path_A$ , which will grow with successive stages.

#### 6.4.1 What will happen if $Path_A$ runs too far ahead of $Path_B$ ?

It is possible that  $Path_A$ 's parallel DIVs finish execution even before  $Path_B$ 's racing stage starts. In this case,  $Path_B$  will no longer suffer from the DIV unit's contention, and the timing difference fails to increase. To solve this problem, we increase the number of operations in the racing stage, so that the limited capacity of the Reorder buffer (ROB) will stop this from occurring. Specifically, when  $Path_B$  has not started, no MUL operation in the same racing stage can release its ROB entry. As long as the number of MUL operations exceeds the ROB capacity, the processor will stall before any parallel DIV can be issued, and can only continue executing in  $Path_A$  after  $Path_B$  also starts its racing stage. This stall only delays  $Path_A$ , so the timing difference will not be affected, as  $Path_B$  is the critical path whose timing is observed.

## 7 Attacks

Here we demonstrate the utility of Hacky Racers, by showing that simple repetition attacks alone do not typically give a timing difference that can be measured, but racing gadgets can fix them. Higher quality, faster bit-rate timers can be created by combining racing gadgets and magnifier gadgets, to allow extremely precise timing (to the nanosecond granularity) to be achieved even with the attack only being

repeated once. Finally we use Hacky Racers to construct a novel backwards-in-time Spectre attack [37], demonstrate its efficacy even in JavaScript, and show how Hacky Racers can be used as a drop-in replacement for SharedArrayBuffer timers [69] by using them to construct LLC eviction sets.

**Processor details** We evaluate on an Intel i7-8750H Coffee Lake processor, though we reproduced similar results when we tried them on an AMD Ryzen 5900HX. The Intel system has 6 physical cores running at 2GHz. Each core has a private 32KB L1 Instruction Cache, 32KB L1 Data Cache, a 256KB L2 cache and a 64-entry L1 TLB. All cores share a 9MB L3 cache and a 1536-entry L2 TLB. The DIVSD instruction has a latency of 13-14 cycles based on the operand content, and 4-cycles reciprocal throughput [24].

Nothing we implement is particularly microarchitecture-specific: our experimental artefact works across all Intel systems we tested out-of-the-box, and only the Prime-And-Scope attack (section 7.4) fails on AMD systems, due to not having support for non-inclusive last-level caches within the underlying side-channel attack (rather than the Hacky Racer). Fundamentally the core needs to be out-of-order (i.e. any contemporary processor except the LITTLE part of Arm's big.LITTLE cores), and some of our individual attacks (but not all Hacky Racers) require either a set-associative cache or some non-fully-pipelined execution units. All of these are ubiquitous. In general we expect some attack-core combinations will require a simple profiling stage within the attacker's JavaScript.

### 7.1 Repetition Gadgets with Racing Gadgets

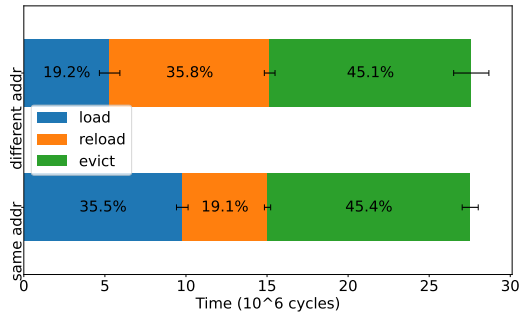
Here we first give an example of how timing difference fails to accumulate by simple repetition [45] of the  $flush+reload$  [92] process. This is an arbitrary choice of attack, chosen to demonstrate that, counter-intuitively, a simple repetition can fail in some circumstances due to attack setup time, unless magnifiers are used to generate coarse timing difference instead.

The load stage will either access the same, or a different, address as the reload stage, which will be evicted in the flush stage. As is shown in figure 7a, although the timing difference accumulates on the reload stage as expected, the loading stage has an opposite timing difference, eliminating the overall timing difference.

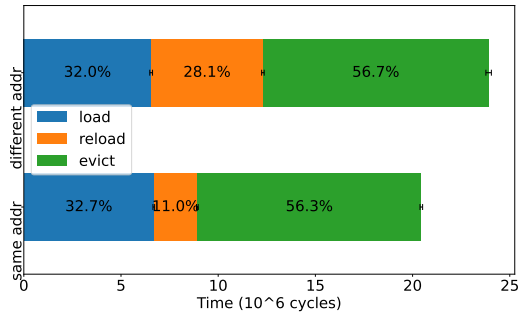
This makes such a simple repetition ineffective as an arbitrary timing gadget; however, Hacky Racers present a solution. We put the load stage into one path of a racing gadget, while the other path's execution time stays constant and always costs more time than the load stage. In this case, the timing difference from the load stage is hidden and the timing side-channel reappears in the total run-time, as is shown in figure 7b.

McIlroy et al. [45] were able to use a repetition gadget to generate Spectre attacks<sup>8</sup>, but the leakage rate is 10B/s, 50× lower than the magnifier-based Spectre attack in section 7.3. This is because most execution time will be timing invariant, and to accumulate a large enough difference from the change in the reload stage alone takes significant time, impacting

<sup>8</sup>The load stage of a Spectre v1 gadget happens inside a misspeculated branch, whose return to correct execution is dictated by the branch-calculation time, which must be longer than the load access. This makes such a construction a racing gadget natively.



(a) Time stack of the full execution of a basic repetition gadget. Without the use of racing gadgets, there is no discernible timing difference across the entire attack, as the cache miss that is saved in one path in the victim load stage is replicated instead in the attacker reload stage.



(b) Time stack of the full execution of an optimized repetition gadget, with a racing gadget used to make the load stage constant-time. The percentages shown are all normalized to the total runtime of the same-address case.

Figure 7: Repetition gadgets need to use racing gadgets in order to show a discernible timing difference.

the bit rate. By combining with a magnifier gadget, we can make almost the entire execution time variant on the secret, increasing bit rates as a result.

This means that the combination of racing and magnifier gadgets are more capable than repetition gadgets alone – as well as providing higher bit rates by making more of the execution time timing-variant: repetition alone is not always sufficient to generate a coarse time signal from an initial fine-grained timing signal. Still, racing gadgets alone are sufficient to improve a repetition gadget’s signal-to-noise ratio, if not achieve high bit rates, by hiding the timing-variant setup time within a timing-invariant racing gadget.

## 7.2 Racing-Gadget Granularity

To test the granularity of *racing gadgets*, we choose the integer add operation to construct the reference path in a Transient P/A Racing Gadget, as each add operation only costs 1 cycle. We pick operations with various latency to construct the target path, and check whether our reference path can distinguish paths with different number of chained operations. The slope of each line is close to ratio between the latency of target operation and reference operation. The granularity is the maximum consecutive points whose Y value stays unchanged, indicating those two target paths cannot be distinguished by their corresponding operation number in the reference path.

For target paths composed of 1-cycle-latency chained operations as well, such as ADD and LEAL instruction shown in figure 8, the granularity is 1 – 3 operations. For MUL

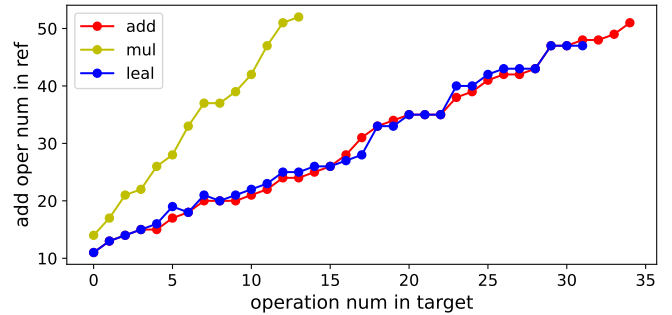


Figure 8: Target operation measured by reference path composed by ADDs. The granularity is the maximum consecutive points that are indistinguishable on the Y axis.

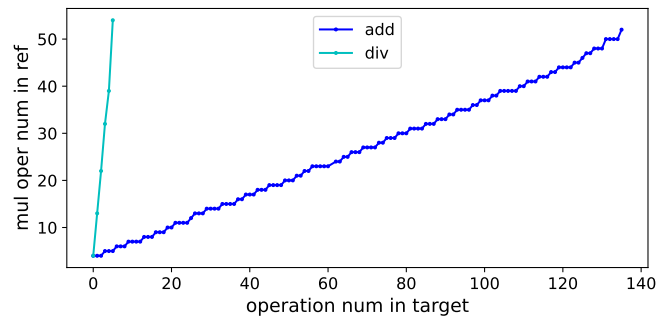


Figure 9: Target operation measured by reference path composed by MULs.

instructions (3-cycle latency), the granularity is 1 – 2 operations. Therefore, the overall minimal granularity of *racing gadgets* is 1 – 6 cycles (0.5 – 3ns). In this particular (Transient P/A) Racing Gadget, all instructions in the ref path are older than those in the target path (as the ref path is a misspeculated branch condition), thus the ROB capacity limits the length of the ref path to 54, which in turn limits the largest execution time that we can time to 54 cycles.

Using MUL operation, whose latency is longer than ADDs, we increase our timer’s maximum timing threshold to around 140 ADD operations, as is shown in Figure 9. However, it sacrifices granularity to around 2 - 4 ADD operations. Still, it can distinguish the number of DIV operations perfectly as DIV’s latency is around 4 times of MUL’s.

## 7.3 Attack: SpectreBack in JavaScript

Rollback-based [64] and other Spectre mitigations that only clean up the effects of misspeculation once it has happened [11, 26, 65] (systems that do not implement strictness order [10]) were broken by attacks [15, 25] that transmit the timing effect via contention. Here we propose a different method of breaking such systems, by transmitting timing information *backwards in time* to a Non-Transient Reorder Racing Gadget (section 5.2) via cache state. It is presented here not only as a user of the reorder racing/magnifier gadgets, but also because the attack *itself* is generated via a custom racing gadget, to transmit it to a reorder racing gadget that exists before any transient execution is squashed. We use the PLRU Magnifier Gadget for Reorder Input to extract

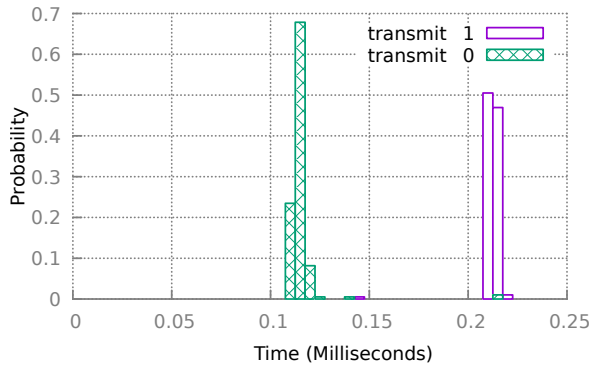


Figure 10: The execution-time distribution after the reorder magnifier access pattern is repeated 4000 times; there is still almost no overlap between the two transmissions.

the secret.

The example code for this gadget is shown in code listing 3. The attacker controls which instruction sequence (line 4 and line 6) completes first based on the value of secret data speculatively accessed at line 8. This timing difference can be converted into the relative access order of array[A] and array[B], similar to a non-transient reorder racing gadget. This order will then be served as the input for the PLRU Gadget for Reorder Input (section 6.2) at line 10. Figure 10 shows the output timing difference of this Gadget when its access pattern is repeated 4000 times.

Similar to leaky.page [62], we use this gadget to leak out-of-bounds array data in Chrome 88, and achieve a 4.3 kilobits/second leakage rate with over 88% accuracy (more than ample to leak secret keys).

```

1 function SpectreBack() {
2   SetInitialCacheState()
3   // access array[A] in the last, array[OFFSET]
   second last
4   temp1 = array[array[a]]
5   // access array[B] in the last, array[OFFSET + 0
   x100] second last
6   temp2 = array[array[b]]
7   // Based on the value of array[x], either access
   array[OFFSET] or array[OFFSET + 0x100]
8   if (x < array_size) {temp3 = array[OFFSET + (((
   array[x]&bitmask) >> bit_num) << 8)]}
9   time_begin = performance.now()
10  traverseMagnifierPattern()
11  time_end = performance.now()
12  return time_end-time_begin;
13 }

```

Code Listing 3: SpectreBack, a new cache-based Spectre backwards-in-time attack. Based on the secret that is speculative accessed at line 8, it will either access `array[OFFSET]` to accelerate line 6, or access `array[OFFSET+0x100]` to accelerate line 4. Therefore, a relative access-order state is left as an input to the magnifier gadget at line 10.

## 7.4 Attack: LLC Eviction-Set Generation

To demonstrate that Hacky Racers can be conveniently utilised by various attacks, we use a combination of the (P/A) Racing Gadget and PLRU Gadget for Presence/Ab-

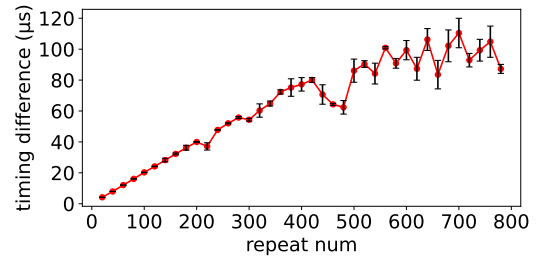


Figure 11: Timing difference magnified by the arbitrary-replacement gadget (section 6.3) with cache-set reuse. Each set is used for contention once and reset to initial state by prefetching within one iteration.

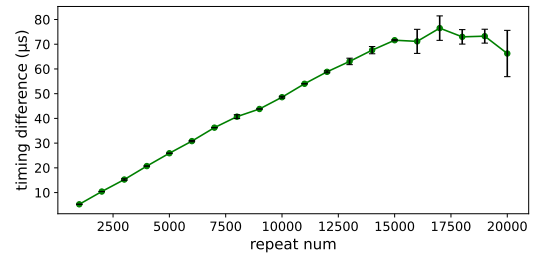


Figure 12: Timing difference magnified by arithmetic operations alone (section 6.4).

sence (P/A) Input as the timer to generate eviction sets (EV), which allow the setup of various other attacks (section 2.2). We use the EV profiling algorithm of Purnal et al. [52], replacing just the timer. Since the timer in this algorithm only needs to distinguish between an *L1 cache hit* and an *L3 cache miss*, composing the reference path in the Racing Gadget with MUL operations can provide a fine enough granularity. We retained their 100% success rate after the timer is replaced by ours. This is just one example that shows Hacky Racers can easily be used to replace existing SharedArray-Buffer timers in JavaScript – and thus resurrects existing attacks even in hardened browsers.

## 7.5 Other Magnifiers

Here we provide a PoC to show how our Arbitrary-Replacement and Arithmetic Gadgets (section 6.3 and 6.4) can also defeat coarsened timers, currently  $5\mu s$ , in browsers.

For the Arbitrary Replacement Gadget, we set half of the L1D cache’s set number, 32, as the set number for each round. We set the prefetch distance as 22 iterations ahead. Figure 11 shows that timing difference accumulates to  $100\mu s$  as we repeatedly traverse through the sets; we also tried the arbitrary replacement gadget without prefetching, but as this was limited by the number of sets in the cache, it could only magnify up to 450 cycles (approximately 225ns).

For the Arithmetic-operation Only Gadget, as is shown in Figure 12, the timing different stops increasing at around a repeat number of 15000. This is because the total run-time approaches the interval of timer interrupts (4ms), and since this magnifier is entirely stateless, it cannot keep accumulating timing difference once the pipeline is reset.

Both of these are more than ample to defeat current timer coarsening. Still, unlike the PLRU-based gadgets, whose magnification rates are almost arbitrary, these magnifiers are

limited to rates close to the maximum ever granularity implemented in a browser (100ms [61]). In practice this is little impediment; both can be combined with repetition gadgets (increasing bit rate compared to repetition alone, by making more of the execution timing-variant, and avoiding any negative correlation with setup time masking the time difference), at the expense of needing the attack to be performed multiple times. Whether either or both can have their magnification rates improved, allowing the attack to be repeated only once even for arbitrarily coarse timers, is open future work.

## 8 Potential Countermeasures

Transient execution is not required for racing or magnifier gadgets: only the transient presence-absence (P/A) racing gadgets in section 5.1 (because they use transient execution directly) and the SpectreBack attack in section 7.3 (because it is a Spectre attack, though it does break Spectre defences [1, 26, 64, 65] that do not guarantee Strictness Order [10], and thus try to clean up misspeculation after it has occurred), use transient execution in any way, and thus only these can be guarded by Spectre defences [4, 10, 11, 26, 34, 64, 65, 66, 84, 93, 94], which are designed to eliminate the negative effects of transient execution. We use transient (P/A) gadgets in many of our examples because they are simple to understand: however, an attacker can easily change to use reorder gadgets instead.

Take DoM [66] (delay-on-miss), a technique which delays cache misses in the L1 until they become non-speculative, and the non-transient reorder racing gadget as an example. The reorder gadget only relies on the relative cache insertion order of two load instructions. Both of these can be entirely non-speculative, and will still race due to instruction-level parallelism, and yet DoM marks them as being safe to execute in any order. To take another example, GhostMinion [10] might change the original L1 cache insertion order by first inserting speculative load into the GhostMinion cache, the exact state that ends up being inserted into the L1 cache still ends up dictated by the out-of-order execution present in the reorder gadget<sup>9</sup>. The fundamental property is that Spectre defences treat transient execution as the dangerous part; and indeed while it is more dangerous than Hacky Racers alone (which leak timing information rather than secrets directly), they do not seek to hide or eliminate channels caused via instruction-level parallelism.

In general, Hacky Racers can be defeated by either preventing the racing gadget’s success in creating the state change, or the magnifier gadget’s success in replicating it – though the attacker may be able to rely on repetition rather than magnification in circumstances where this still provides a high enough signal-to-noise ratio (section 7.1). Some of our magnifiers are limited in magnification capability, and could be defeated via further coarsening (section 7.5), whereas others (the PLRU gadgets) are unlikely to be

limited without removing any source of coarse-grained time completely, which is likely to be impossible in practice. We expect coarser-grained magnifiers not using PLRU to follow, and even our least effective magnifiers would still combine well with repetition in such an environment.

One potential way to completely mitigate the cache-based reorder gadget we give in this paper is to guarantee cache state is always equivalent to an in-order execution. We leave the design, evaluation and overheads (and whether such overheads are feasible for deployment, given the existing overheads of Spectre defences without such guarantees) of such a scheme to future work. Likewise, our reorder magnifier is based on PLRU replacement, and so other policies will break this specific gadget, though we present others that translate over simply. But even if this cache-based gadget is mitigated, an attacker can then change strategy to transmit timing based on within-core contention – where in the general case, assuring behavior equivalent to in-order execution is likely to require actual in-order execution.

For run-time detection mechanisms [12, 17, 20, 50, 95], we expect racing gadgets to look so similar to normal out-of-order execution that they will be difficult to catch without very high false positive rates. Still, since magnifier gadgets rely on highly repetitive patterns, detection of at least high-bitrate channels may be feasible, but will require different schemes for every possible repeated pattern, and so attackers will keep changing strategy. Frequent L1 cache misses exists in PLRU gadget of section 6.1 and Arbitrary Replacement Gadget in section 6.3, therefore the L1 cache miss counter could be utilized to as one input to such a detector, though only as a very weak classifier. Similar to the port contention attack by Rokicki et al. [60], the Arithmetic-Operation-Only Gadget of section 6.4 executes long backend-bounded instruction (arithmetic operations) chain without misprediction, which makes the ratio of backend-bound execution divided by misprediction-bound execution also a potential parameter to detect this gadget. Besides, since this attack also requires precise instruction sequence construction like that by Rokicki et al. [60], the reordering of instruction sequences from either browser’s optimization or software-diversification [23, 55] can affect the efficiency of Hacky Racers, and software analysis [85] within JavaScript compilers may be able to pick up attacks that are less well obfuscated. Still, in some scenarios attackers may have enough control to manually construct the instruction sequence or implement multiple backup sequences to overcome any such analysis. Again, we leave this for future study.

For browser security, where the main threats are from making Spectre and fingerprinting attacks simpler even without SharedArrayBuffer timers, cross-origin isolation policies [36] (as opposed to site isolation alone which was attacked by spook.js [8]) move many targets outside the address space, although implementation requires manual effort to avoid breaking compatibility, and so adoption is not yet universal. A similar process-level isolation policy [71] is needed in Cloudflare, otherwise Hacky Racers will make the Spectre-attack proposed by Martin et al. [71] much easier. We also believe that Tor, which currently disables *SharedArrayBuffer* even with cross-origin isolation [2], now gains very limited protection from this constraint, in the presence of Hacky Racers.

<sup>9</sup>The strictness order presented in GhostMinion [10] does not guarantee the cache state of the L1 is always equivalent to an in-order execution. While it ensures that a less speculative instruction cannot see out-of-order execution of a more speculative instruction, it does not guarantee the opposite, as that is not necessary to hide transient execution. So a load at timestamp 21 may validly be evicted from the GhostMinion by a load at timestamp 20 if the latter happened afterwards in out-of-order execution – meaning that only load 20 ends up in the L1 cache after – whereas if they were executed in program order, both may reach the L1 in sequence.

## 9 Discussion and Conclusion

Hacky Racers show that high-resolution timing information can be extracted via instruction-level parallelism, even in highly restricted JavaScript environments, and even without multiple threads [69] or any language features that could realistically be disabled. We do not believe mitigation to be particularly realistic; out-of-order execution is vital for single-threaded performance (so systems will not be going in-order), removal of PLRU cache replacement [33] will only cause the attacker to change strategy, and while some of our gadgets could be eliminated through further coarsening, others work to almost arbitrary degree, and all can be amplified further by repetition. We also expect further magnifiers to follow. This demonstrates that timer coarsening has limited efficacy in any browser security model, and the removal of SharedArrayBuffer from sites without cross-site isolation [13] in Chrome and Firefox is insufficient to protect them from timing side channels. Threats will have to be dealt with, in future, by isolation [57] only. Hacky Racers may also impact other security models with restricted timing, such as the removal of user-privilege fine-grained timers on M1 processors and other ARM systems [41, 56]; we leave consideration of these to future work.

Our attacks also have implications for architects. While Spectre [37] showed speculative execution to be a fundamental source of information leakage, Hacky Racers goes even further: even correct execution results in information leakage. Is any microarchitectural performance optimisation truly secure, given the right threat model?

## 10 Acknowledgement

We would like to sincerely thank ASPLOS 2023 Reviewers for your helpful feedback. We would also like to thank Thomas Rokicki for providing a modified version of Chromium.

## References

- [1] <https://gitlab.torproject.org/tpo/applications/tor-browser/-/issues/16110>.
- [2] <https://gitlab.torproject.org/tpo/applications/tor-browser/-/issues/40016>.
- [3] Mitigating side-channel attacks. <https://www.chromium.org/Home/chromium-security/ssca/>, 2018.
- [4] Invispec-1.0 simulator bug fix. <https://github.com/mjyan0720/InvisiSpec-1.0/commit/f29164ba510b92397a26d8958fd87c0a2b636b0c>, 2019.
- [5] cloudflare workers, 2022.
- [6] High resolution time. <https://www.w3.org/TR/hr-time/>, 2022.
- [7] timer in chrome. <https://chromestatus.com/feature/6497206758539264>, 2022.
- [8] Ayush Agarwal, Sioli O’Connell, Jason Kim, Shaked Yehezkel, Daniel Genkin, Eyal Ronen, and Yuval Yarom. Spook.js: Attacking chrome strict site isolation via speculative execution. In *2022 IEEE Symposium on Security and Privacy (SP)*, 2022.
- [9] Pavlos Aimoniotis, Christos Sakalis, Magnus Sjölander, and Stefanos Kaxiras. “It’s a trap!”—how speculation invariance can be abused with forward speculative interference. *arXiv preprint arXiv:2109.10774*, 2021.
- [10] Sam Ainsworth. Ghostminion: A strictness-ordered cache system for spectre mitigation. In *MICRO-54: 54th Annual IEEE/ACM International Symposium on Microarchitecture*, pages 592–606, 2021.
- [11] Sam Ainsworth and Timothy M Jones. Muontrap: Preventing cross-domain spectre-like attacks by capturing speculative state. In *2020 ACM/IEEE 47th Annual International Symposium on Computer Architecture (ISCA)*, pages 132–144. IEEE, 2020.
- [12] Manaar Alam, Sarani Bhattacharya, Debdeep Mukhopadhyay, and Sourangshu Bhattacharya. Performance counters to rescue: A machine learning based safeguard against micro-architectural side-channel-attacks. *Cryptology ePrint Archive*, 2017.
- [13] Jake Archibald and Eiji Kitamura. <https://developer.chrome.com/blog/enabling-shared-array-buffer/>, 2022.
- [14] ARM Limited. Arm1176jzf-s technical reference manual. [Online; accessed 23-October-2022].
- [15] Mohammad Behnia, Prateek Sahu, Riccardo Paccagnella, Jiyong Yu, Zirui Neil Zhao, Xiang Zou, Thomas Unterluggauer, Josep Torrellas, Carlos Rozas, Adam Morrison, et al. Speculative interference attacks: Breaking invisible speculation schemes. In *Proceedings of the 26th ACM International Conference on Architectural Support for Programming Languages and Operating Systems*, pages 1046–1060, 2021.
- [16] Atri Bhattacharyya, Alexandra Sandulescu, Matthias Neugschwandtner, Alessandro Sorniotti, Babak Falsafi, Mathias Payer, and Anil Kurmus. Smotherspectre: exploiting speculative execution through port contention. In *Proceedings of the 2019 ACM SIGSAC Conference on Computer and Communications Security*, pages 785–800, 2019.
- [17] Samira Briongos, Gorka Irazoqui, Pedro Malagón, and Thomas Eisenbarth. Cacheshield: Detecting cache attacks through self-observation. In *Proceedings of the Eighth ACM Conference on Data and Application Security and Privacy*, pages 224–235, 2018.
- [18] Samira Briongos, Pedro Malagón, José M Moya, and Thomas Eisenbarth. RELOAD+ REFRESH: Abusing cache replacement policies to perform stealthy cache attacks. In *29th USENIX Security Symposium (USENIX Security 20)*, pages 1967–1984, 2020.
- [19] Claudio Canella, Daniel Genkin, Lukas Giner, Daniel Gruss, Moritz Lipp, Marina Minkin, Daniel Moghimi, Frank Piessens, Michael Schwarz, Berk Sunar, et al. Fallout: Leaking data on meltdown-resistant cpus. In *Proceedings of the 2019 ACM SIGSAC Conference on Computer and Communications Security*, pages 769–784, 2019.
- [20] Marco Chiappetta, Erkay Savas, and Cemal Yilmaz. Real time detection of cache-based side-channel attacks using hardware performance counters. *Applied Soft Computing*, 49:1162–1174, 2016.
- [21] MDN contributors. Sharedarraybuffer. [https://developer.mozilla.org/en-US/docs/Web/JavaScript/Reference/Global\\_Objects/SharedArrayBuffer](https://developer.mozilla.org/en-US/docs/Web/JavaScript/Reference/Global_Objects/SharedArrayBuffer), 2022.
- [22] Bart Coppens, Ingrid Verbauwhede, Koen De Bosschere, and Bjorn De Sutter. Practical mitigations for timing-based side-channel attacks on modern x86 processors. In *2009 30th IEEE symposium on security and privacy*, pages 45–60. IEEE, 2009.
- [23] Stephen Crane, Andrei Homescu, Stefan Brunthaler, Per Larsen, and Michael Franz. Thwarting cache side-channel attacks through dynamic software diversity. In *NDSS*, pages 8–11, 2015.
- [24] Agner Fog. Instruction tables: Lists of instruction latencies, throughputs and micro-operation breakdowns for intel, amd and via cpus. [https://www.agner.org/optimize/instruction\\_tables.pdf](https://www.agner.org/optimize/instruction_tables.pdf), 2022.
- [25] Jacob Fustos, Michael Bechtel, and Heechul Yun. Spectrerewind: Leaking secrets to past instructions. In *Proceedings of the 4th ACM Workshop on Attacks and Solutions in Hardware Security*, pages 117–126, 2020.
- [26] Abraham Gonzalez, Ben Korpan, Jerry Zhao, Ed Younis, and Krste Asanović. Replicating and mitigating Spectre attacks on an open source RISC-V microarchitecture. In *CARRV*, 2019.
- [27] Ben Gras, Kaveh Razavi, Erik Bosman, Herbert Bos, and Cristiano Giuffrida. ASLR on the line: Practical cache attacks on the mmu. In *NDSS*, volume 17, page 26, 2017.
- [28] Daniel Gruss, Clémentine Maurice, Anders Fogh, Moritz Lipp, and Stefan Mangard. Prefetch side-channel attacks: Bypassing smap and kernel aslr. In *Proceedings of the 2016 ACM SIGSAC conference on computer and communications security*, pages 368–379, 2016.

- [29] Daniel Gruss, Clémentine Maurice, and Stefan Mangard. Rowhammer.js: A remote software-induced fault attack in javascript. In *International conference on detection of intrusions and malware, and vulnerability assessment*, pages 300–321. Springer, 2016.
- [30] Daniel Gruss, Raphael Spreitzer, and Stefan Mangard. Cache template attacks: Automating attacks on inclusive last-level caches. In *24th USENIX Security Symposium (USENIX Security 15)*, pages 897–912, 2015.
- [31] ECMA International. ECMAScript 2017 language specification. [https://www.ecma-international.org/wp-content/uploads/ECMA-262\\_8th\\_edition\\_june\\_2017.pdf](https://www.ecma-international.org/wp-content/uploads/ECMA-262_8th_edition_june_2017.pdf), 2017.
- [32] Gorka Irazoqui, Thomas Eisenbarth, and Berk Sunar. S \$ a: A shared cache attack that works across cores and defies vm sandboxing—and its application to aes. In *2015 IEEE Symposium on Security and Privacy*, pages 591–604. IEEE, 2015.
- [33] Kamil Kedzierski, Miquel Moreto, Francisco J Cazorla, and Mateo Valero. Adapting cache partitioning algorithms to pseudo-lru replacement policies. In *2010 IEEE International Symposium on Parallel & Distributed Processing (IPDPS)*, pages 1–12. IEEE, 2010.
- [34] Khaled N Khasawneh, Esmail Mohammadian Koruyeh, Chengyu Song, Dmitry Evtushkin, Dmitry Ponomarev, and Nael Abu-Ghazaleh. Safespec: Banishing the spectre of a meltdown with leakage-free speculation. In *2019 56th ACM/IEEE Design Automation Conference (DAC)*, pages 1–6. IEEE, 2019.
- [35] Vladimir Kiriansky and Carl Waldspurger. Speculative buffer overflows: Attacks and defenses. *arXiv preprint arXiv:1807.03757*, 2018.
- [36] Eiji Kitamura and Domenic Denicola. Why you need “cross-origin isolated” for powerful features. <https://web.dev/why-coop-coep/>, 2021.
- [37] Paul Kocher, Jann Horn, Anders Fogh, Daniel Genkin, Daniel Gruss, Werner Haas, Mike Hamburg, Moritz Lipp, Stefan Mangard, Thomas Prescher, et al. Spectre attacks: Exploiting speculative execution. In *2019 IEEE Symposium on Security and Privacy (SP)*, pages 1–19. IEEE, 2019.
- [38] David Kohlbrenner and Hovav Shacham. Trusted browsers for uncertain times. In *25th USENIX Security Symposium (USENIX Security 16)*, pages 463–480, 2016.
- [39] Esmail Mohammadian Koruyeh, Khaled N Khasawneh, Chengyu Song, and Nael Abu-Ghazaleh. Spectre returns! speculation attacks using the return stack buffer. In *12th USENIX Workshop on Offensive Technologies (WOOT 18)*, 2018.
- [40] Moritz Lipp, Daniel Gruss, and Michael Schwarz. AMD prefetch attacks through power and time. In *31st USENIX Security Symposium (USENIX Security 22)*, 2022.
- [41] Moritz Lipp, Daniel Gruss, Raphael Spreitzer, Clémentine Maurice, and Stefan Mangard. {ARMageddon}: Cache attacks on mobile devices. In *25th USENIX Security Symposium (USENIX Security 16)*, pages 549–564, 2016.
- [42] Moritz Lipp, Michael Schwarz, Daniel Gruss, Thomas Prescher, Werner Haas, Anders Fogh, Jann Horn, Stefan Mangard, Paul Kocher, Daniel Genkin, Yuval Yarom, and Mike Hamburg. Meltdown: Reading kernel memory from user space. In *27th USENIX Security Symposium (USENIX Security 18)*, 2018.
- [43] Fangfei Liu, Yuval Yarom, Qian Ge, Gernot Heiser, and Ruby B Lee. Last-level cache side-channel attacks are practical. In *2015 IEEE symposium on security and privacy*, pages 605–622. IEEE, 2015.
- [44] Giorgi Maisuradze and Christian Rossow. ret2spec: Speculative execution using return stack buffers. In *Proceedings of the 2018 ACM SIGSAC Conference on Computer and Communications Security*, pages 2109–2122, 2018.
- [45] Ross McIlroy, Jaroslav Sevcik, Tobias Tebbi, Ben L Titzer, and Toon Verwaest. Spectre is here to stay: An analysis of side-channels and speculative execution. *arXiv preprint arXiv:1902.05178*, 2019.
- [46] MDN Contributors. high resolution time. [https://developer.mozilla.org/en-US/docs/Web/API/Performance\\_API](https://developer.mozilla.org/en-US/docs/Web/API/Performance_API), 2022.
- [47] MDN Contributors. performance.now(). <https://developer.mozilla.org/en-US/docs/Web/API/Performance/now>, 2022.
- [48] Yossef Oren, Vasileios P Kemerlis, Simha Sethumadhavan, and Angelos D Keromytis. The spy in the sandbox: Practical cache attacks in javascript and their implications. In *Proceedings of the 22nd ACM SIGSAC Conference on Computer and Communications Security*, pages 1406–1418, 2015.
- [49] Dag Arne Osvik, Adi Shamir, and Eran Tromer. Cache attacks and countermeasures: the case of aes. In *Cryptographers’ track at the RSA conference*, pages 1–20. Springer, 2006.
- [50] Mathias Payer. Hexpads: a platform to detect “stealth” attacks. In *International Symposium on Engineering Secure Software and Systems*, pages 138–154. Springer, 2016.
- [51] Colin Percival. Cache missing for fun and profit, 2005.
- [52] Antoon Purnal, Furkan Turan, and Ingrid Verbauwhede. Prime+ scope: Overcoming the observer effect for high-precision cache contention attacks. In *Proceedings of the 2021 ACM SIGSAC Conference on Computer and Communications Security*, pages 2906–2920, 2021.
- [53] Antoon Purnal, Furkan Turan, and Ingrid Verbauwhede. Double trouble: Combined heterogeneous attacks on Non-Inclusive cache hierarchies. In *31st USENIX Security Symposium (USENIX Security 22)*, Boston, MA, August 2022. USENIX Association.
- [54] Hany Ragab, Enrico Barberis, Herbert Bos, and Cristiano Giuffrida. Rage against the machine clear: A systematic analysis of machine clears and their implications for transient execution attacks. In *30th USENIX Security Symposium (USENIX Security 21)*, pages 1451–1468, 2021.
- [55] Ashay Rane, Calvin Lin, and Mohit Tiwari. Raccoon: Closing digital {Side-Channels} through obfuscated execution. In *24th USENIX Security Symposium (USENIX Security 15)*, pages 431–446, 2015.
- [56] Joseph Ravichandran, Weon Taek Na, Jay Lang, and Mengjia Yan. Pacman: attacking arm pointer authentication with speculative execution. In *ISCA*, pages 685–698, 2022.
- [57] Charles Reis, Alexander Moshchuk, and Nasko Oskov. Site isolation: Process separation for web sites within the browser. In *28th USENIX Security Symposium (USENIX Security 19)*, pages 1661–1678, 2019.
- [58] Xida Ren, Logan Moody, Mohammadkazem Taram, Matthew Jordan, Dean M Tullsen, and Ashish Venkat. I see dead μops: Leaking secrets via intel/amd micro-op caches. In *2021 ACM/IEEE 48th Annual International Symposium on Computer Architecture (ISCA)*, pages 361–374. IEEE, 2021.
- [59] Vera Rimmer, Davy Preuveneers, Marc Juarez, Tom Van Goethem, and Wouter Joosen. Automated website fingerprinting through deep learning. *arXiv preprint arXiv:1708.06376*, 2017.
- [60] Thomas Rokicki, Clémentine Maurice, and Michael Schwarz. Cpu port contention without smt. In *European Symposium on Research in Computer Security*, pages 209–228. Springer, 2022.
- [61] Thomas Rokicki, Clémentine Maurice, and Pierre Laperdrix. Sok: In search of lost time: A review of javascript timers in browsers. In *2021 IEEE European Symposium on Security and Privacy (EuroS P)*, pages 472–486, 2021.
- [62] Stephen Röttger and Artur Janc. A spectre proof-of-concept for a spectre-proof web. <https://leaky.page/blog>, 2021.
- [63] Gururaj Saileshwar, Christopher W Fletcher, and Moinuddin Qureshi. Streamline: a fast, flushless cache covert-channel attack by enabling asynchronous collusion. In *Proceedings of the 26th ACM International Conference on Architectural Support for Programming Languages and Operating Systems*, pages 1077–1090, 2021.
- [64] Gururaj Saileshwar and Moinuddin K Qureshi. Cleanupspec: An “undo” approach to safe speculation. In *Proceedings of the 52nd Annual IEEE/ACM International Symposium on Microarchitecture*, pages 73–86, 2019.
- [65] Christos Sakalis, Mehdi Alipour, Alberto Ros, Alexandra Jimborean, Stefanos Kaxiras, and Magnus Själander. Ghost loads: What is the cost of invisible speculation? In *Proceedings of the 16th ACM International Conference on Computing Frontiers*, CF ’19, page 153–163, New York, NY, USA, 2019. Association for Computing Machinery.
- [66] Christos Sakalis, Stefanos Kaxiras, Alberto Ros, Alexandra Jimborean, and Magnus Själander. Efficient invisible speculative execution through selective delay and value prediction. In *2019 ACM/IEEE 46th Annual International Symposium on Computer Architecture (ISCA)*, pages 723–735. IEEE, 2019.

- [67] Michael Schwarz, Moritz Lipp, and Daniel Gruss. JavaScript Zero: Real JavaScript and zero side-channel attacks. In *NDSS*, volume 18, page 12, 2018.
- [68] Michael Schwarz, Moritz Lipp, Daniel Moghimi, Jo Van Bulck, Julian Stecklina, Thomas Prescher, and Daniel Gruss. Zombieload: Cross-privilege-boundary data sampling. In *Proceedings of the 2019 ACM SIGSAC Conference on Computer and Communications Security*, pages 753–768, 2019.
- [69] Michael Schwarz, Clémentine Maurice, Daniel Gruss, and Stefan Mangard. Fantastic timers and where to find them: High-resolution microarchitectural attacks in javascript. In *International Conference on Financial Cryptography and Data Security*, pages 247–267. Springer, 2017.
- [70] Michael Schwarz, Martin Schwarzl, Moritz Lipp, Jon Masters, and Daniel Gruss. Netspectre: Read arbitrary memory over network. In *European Symposium on Research in Computer Security*, pages 279–299. Springer, 2019.
- [71] Martin Schwarzl, Pietro Borrello, Andreas Kogler, Kenton Varda, Thomas Schuster, Daniel Gruss, and Michael Schwarz. Dynamic process isolation. *arXiv preprint arXiv:2110.04751*, 2021.
- [72] Anatoly Shusterman, Ayush Agarwal, Sioli O’Connell, Daniel Genkin, Yossi Oren, and Yuval Yarom. Prime+ Probe 1, JavaScript 0: Overcoming browser-based side-channel defenses. In *30th USENIX Security Symposium (USENIX Security 21)*, pages 2863–2880, 2021.
- [73] Anatoly Shusterman, Lachlan Kang, Yarden Haskal, Yosef Meltser, Prateek Mittal, Yossi Oren, and Yuval Yarom. Robust website fingerprinting through the cache occupancy channel. In *28th USENIX Security Symposium (USENIX Security 19)*, pages 639–656, 2019.
- [74] Dimitrios Skarlatos, Mengjia Yan, Bhargava Gopireddy, Read Sprabery, Josep Torrellas, and Christopher W Fletcher. Microscope: Enabling microarchitectural replay attacks. In *2019 ACM/IEEE 46th Annual International Symposium on Computer Architecture (ISCA)*, pages 318–331. IEEE, 2019.
- [75] Wei Song and Peng Liu. Dynamically finding minimal eviction sets can be quicker than you think for side-channel attacks against the LLC. In *22nd International Symposium on Research in Attacks, Intrusions and Defenses (RAID 2019)*, pages 427–442, 2019.
- [76] Paul Stone. Pixel perfect timing attacks with html5. *Context Information Security (White Paper)*, 2013.
- [77] Y. Tobah, A. Kwong, I. Kang, D. Genkin, and K. G. Shin. Spechammer: Combining spectre and rowhammer for new speculative attacks. In *2022 IEEE Symposium on Security and Privacy (SP)*, pages 1362–1379. IEEE, 2022.
- [78] Po-An Tsai, Andres Sanchez, Christopher W Fletcher, and Daniel Sanchez. Safecracker: Leaking secrets through compressed caches. In *Proceedings of the Twenty-Fifth International Conference on Architectural Support for Programming Languages and Operating Systems*, pages 1125–1140, 2020.
- [79] Jo Van Bulck, Marina Minkin, Ofir Weisse, Daniel Genkin, Baris Kasikci, Frank Piessens, Mark Silberstein, Thomas F Wenisch, Yuval Yarom, and Raoul Strackx. Foreshadow: Extracting the keys to the intel SGX kingdom with transient out-of-order execution. In *27th USENIX Security Symposium (USENIX Security 18)*, pages 991–1008, 2018.
- [80] Tom Van Goethem, Wouter Joosen, and Nick Nikiforakis. The clock is still ticking: Timing attacks in the modern web. In *Proceedings of the 22nd ACM SIGSAC Conference on Computer and Communications Security*, pages 1382–1393, 2015.
- [81] Stephan Van Schaik, Alyssa Milburn, Sebastian Österlund, Pietro Frigo, Giorgi Maisuradze, Kaveh Razavi, Herbert Bos, and Cristiano Giuffrida. Ridl: Rogue in-flight data load. In *2019 IEEE Symposium on Security and Privacy (SP)*, pages 88–105. IEEE, 2019.
- [82] Bhanu C Vattikonda, Sambit Das, and Hovav Shacham. Eliminating fine grained timers in Xen. In *Proceedings of the 3rd ACM workshop on Cloud computing security workshop*, pages 41–46, 2011.
- [83] Pepe Vila, Boris Köpf, and José F Morales. Theory and practice of finding eviction sets. In *2019 IEEE Symposium on Security and Privacy (SP)*, pages 39–54. IEEE, 2019.
- [84] Ofir Weisse, Ian Neal, Kevin Loughlin, Thomas F Wenisch, and Baris Kasikci. Nda: Preventing speculative execution attacks at their source. In *Proceedings of the 52nd Annual IEEE/ACM International Symposium on Microarchitecture*, pages 572–586, 2019.
- [85] Jan Wichelmann, Florian Sieck, Anna Pätschke, and Thomas Eisenbarth. Microwalk-ci: Practical side-channel analysis for javascript applications. 2022.
- [86] Johannes Wikner, Cristiano Giuffrida, Herbert Bos, and Kaveh Razavi. Spring: Spectre Returning in the Browser with Speculative Load Queuing and Deep Stacks. In *WOOT*, May 2022.
- [87] Wenjie Xiong and Jakub Szefer. Leaking information through cache lru states. In *2020 IEEE International Symposium on High Performance Computer Architecture (HPCA)*, pages 139–152. IEEE, 2020.
- [88] Mengjia Yan, Jiho Choi, Dimitrios Skarlatos, Adam Morrison, Christopher Fletcher, and Josep Torrellas. Invisispec: Making speculative execution invisible in the cache hierarchy. In *2018 51st Annual IEEE/ACM International Symposium on Microarchitecture (MICRO)*, pages 428–441, 2018.
- [89] Mengjia Yan, Christopher W Fletcher, and Josep Torrellas. Cache telepathy: Leveraging shared resource attacks to learn DNN architectures. In *29th USENIX Security Symposium (USENIX Security 20)*, pages 2003–2020, 2020.
- [90] Mengjia Yan, Read Sprabery, Bhargava Gopireddy, Christopher Fletcher, Roy Campbell, and Josep Torrellas. Attack directories, not caches: Side channel attacks in a non-inclusive world. In *2019 IEEE Symposium on Security and Privacy (SP)*, pages 888–904. IEEE, 2019.
- [91] Guo Yanan, Xin Xin, Zhang Youtao, and Jun Yang. eaky way: A conflict-based cache covert channel bypassing set associativity. In *Proceedings of the 55nd Annual IEEE/ACM International Symposium on Microarchitecture*, 2022.
- [92] Yuval Yarom and Katrina Falkner. FLUSH+ RELOAD: A high resolution, low noise, L3 cache side-channel attack. In *23rd USENIX Security Symposium (USENIX Security 14)*, pages 719–732, 2014.
- [93] Jiyong Yu, Namrata Mantri, Josep Torrellas, Adam Morrison, and Christopher W Fletcher. Speculative data-oblivious execution: Mobilizing safe prediction for safe and efficient speculative execution. In *2020 ACM/IEEE 47th Annual International Symposium on Computer Architecture (ISCA)*, pages 707–720. IEEE, 2020.
- [94] Jiyong Yu, Mengjia Yan, Artem Khyzha, Adam Morrison, Josep Torrellas, and Christopher W Fletcher. Speculative taint tracking (stt): a comprehensive protection for speculatively accessed data. In *Proceedings of the 52nd Annual IEEE/ACM International Symposium on Microarchitecture*, pages 954–968, 2019.
- [95] Tianwei Zhang, Yinqian Zhang, and Ruby B Lee. Cloudradar: A real-time side-channel attack detection system in clouds. In *International Symposium on Research in Attacks, Intrusions, and Defenses*, pages 118–140. Springer, 2016.